On water reorientation dynamics in cation hydration shells

Eva Pluhařová,[†,¶] Guillaume Stirnemann,[*,‡] and Damien Laage[*,†]

†*PASTEUR, Department of Chemistry, École Normale Supérieure, PSL University, Sorbonne Université, CNRS 75005, Paris, France*

‡*CNRS Laboratoire de Biochimie Théorique, Institut de Biologie Physico-Chimique, PSL University, Université de Paris, 13 rue Pierre et Marie Curie, 75005, Paris, France*

¶*Present address: J. Heyrovský Institute of Physical Chemistry, Czech Academy of Sciences, Dolejskova 2155/3, 182 23 Prague, Czech Republic*

E-mail: stirnemann@ibpc.fr; damien.laage@ens.psl.edu

Abstract

The effects of ions on liquid water's structural, dynamical, and thermodynamical properties have key implications for a wide range of biological and technological processes. Based on simulations and analytic modeling, we have recently developed a framework that allows to rationalize the effects of solutes and interfaces on water reorientation dynamics. However, this picture still misses some contributions of the cations to the experimentally measured slowdown or acceleration of water dynamics. All-atom classical simulations also face some limitations in quantitatively reproducing water structural and dynamical features in ionic aqueous solutions. Here, we show that a scaled-charge approach can successfully reproduce experimental trends and that ab-initio descriptions are not required. We show that a picture where the cation would lock a water molecule dipole and lead to partial OH reorientation is both incorrect for some ions, and largely exaggerated for others. We demonstrate that a combination of two effects on the hydrogen-bond (H-bond) exchange dynamics allows to understand the ambient temperature acceleration of water reorientation next to a cesium cation, and the retardation next to lithium and magnesium cations. First, ions create a local excluded volume, which hinders the approach of possible new H-bond partners, leading to a retarding contribution. However, they also perturb the local water structure, reducing the energetic cost of elongating the initial H-bond. For magnesium and lithium cations, the excluded volume effect dominates, which leads to an overall retardation of the H-bond exchange. For the cesium cation, at room temperature, this latter contribution overcomes the excluded volume effect, leading to an acceleration; moreover, the strong temperature dependence observed in the experiments, going from a large acceleration close to freezing to a retardation close to boiling, is understood by the key enthalpic effect of the elongation contribution. Overall, our framework now allows to reach a comprehensive understanding of cations' and anions' effects on water reorientation dynamics.

Introduction

Due to its polar character, water can readily dissolve charged species, and atomic and small molecular ions are typically soluble in liquid water up to very high concentrations. For example, each 100 mL of water can accommodate up to 36 grams of table salt at ambient temperature. Most of the water present in our environment or within our cells therefore contains ions. More than 97% of the earth's water is found in oceans as salt water, and even fresh water from the "purest" water springs contains a substantial amount of dissolved ions. The solubility and transport of these ions in aqueous solutions are central to many biochemical and geological processes, and have major technological implications, including, e.g., for the development of new electrolytes for batteries.

The presence of ions affects both the structure and the dynamics of aqueous ionic solutions.[1] The ions' impact on water dynamics has been characterized via a range of experimental techniques which probe several complementary aspects of the solution's dynamics, including dielectric relaxation,[2] viscosity,[3] and molecular reorientation of water probed by NMR and nonlinear vibrational spectroscopies.[1,2,4–6] Experimental measurements and numerical simulations have shown[1,2,4–9] that the effect of ions on water dynamics depends on the nature of the anion and cation, on their concentration, and on the dynamical quantity being probed. For example, some salts have been found to accelerate the dynamics of water while others slow it down, and the same salt can have opposite effects on the dynamics of water depending on whether it is present in dilute or concentrated conditions.

Understanding the molecular-level properties which govern the ions' impact on the solution dynamics has thus been a long-standing question. Recent work in our group has established that water reorientation dynamics mainly proceeds via angular jumps which occur when a water OH group exchanges hydrogen(H)-bond acceptors.[10,11] This extended jump model combines analytic modeling and atomistic molecular dynamics simulations and was shown to provide a molecular understanding of water reorientation dynamics in a broad range of aqueous systems,[12,13] including ionic aqueous solutions.[7,8,14,15] For example, this

model revealed[8] the key role played by the strength of anion-water H-bonds in determining the dynamics: in dilute conditions, anions which accept strong H-bonds from water tend to slow down H-bond exchanges and thus the water reorientation dynamics, while anions which form weak H-bonds can accelerate water dynamics. In concentrated solutions, additional crowding effects were shown to lead to a slowdown for all salts,[7,8,15] in agreement with experiments.[5] Note that extreme concentrations, for which the water to salt ratio goes below the typical hydration shell size in dilute solutions, can lead to additional slowdown effects.[16]

However, the jump picture has so far focused on the effect of anions on water dynamics, and a comparable understanding is missing for the impact of cations. An important difference between anions and cations is that the former accept H-bonds from water whose strength is key to determine the magnitude of the induced acceleration or slowdown,[17] while the latter do not engage in H-bonds with water and mainly interact electrostatically with the negative charge on the water oxygen atoms. It has been suggested[2] that cations affect water dynamics by "locking" the orientation of surrounding water molecules' dipoles via the cation electrostatic field. However, this picture seems to be overly simplified since neutron scattering experiments and simulations have shown that the orientation of water molecules within the hydration shell of cations exhibits an important angular dispersion,[8,18] and it fails to explain the acceleration of water reorientation dynamics measured experimentally for some large cations including, e.g., Cs^+.[5,6]

Our present contribution aims at filling that gap in the understanding of cations' effects on water dynamics by specifically addressing the molecular mechanism behind water acceleration next to Cs^+, and contrasting it with the slowdown measured for other cations such as Li^+ and Mg^{2+}. We use molecular dynamics simulations which have already been successfully employed to elucidate how anions affect water reorientation dynamics.[7,8,14,15] However, for cations, traditional classical forcefields have been shown to fail to reproduce the experimentally observed acceleration of water dynamics induced by some large cations,[19–21] and it has been suggested that density functional theory(DFT)-based simulations[21] or simula-

tions explicitly accounting for cation-water charge transfer [22] are required. Here we performed both DFT-based simulations and classical non-polarizable simulations with a rescaled-cation charge (ECC) approach. We show that both strategies reproduce the acceleration of water dynamics next to Cs^+, but that the reduced computational cost of scaled-charge simulations allows for a more extensive sampling and better convergence. Our scaled-charge simulations further reveal the pronounced anisotropy of water reorientation induced by the Cs^+, Li^+ and Mg^{2+} cations, which is consistent with NMR measurements but cannot be satisfactorily described by the "locking" picture of the water dipole by the cation. [2] We then determine the molecular impact of cations on water reorientation dynamics. We demonstrate that the combination of two effects on the H-bond exchange dynamics allows to understand the ambient temperature acceleration of water reorientation next to Cs^+ and the retardation next to Li^+ and Mg^{2+}, as well as the strong temperature dependence observed experimentally for water dynamics in the Cs^+ hydration shell.

Methods

Simulation strategy and models

A well known limitation of traditional classical cation forcefields is their failure to reproduce the accelerated dynamics (e.g., enhanced water diffusion and decreased water viscosity) observed experimentally for some ions. [19–21] A similar difficulty was also found for some polarizable models. [20] Classical forcefields were shown to lead to a retardation of water dynamics for all investigated cations, including Cs^+, [19–21] which therefore contrasts with the acceleration that has been measured by several techniques for this dilute cation. This has led to the suggestion that DFT-based MD [21] or simulations accounting for charge transfer [22] are required. However, another promising approach relies on scaled ion charges, [23,24] that implicitly account for the fast electronic dielectric response of water. This electronic continuum correction (ECC) strategy has been first successfully employed to reproduce structural

features of aqueous ionic solutions.[25–28] We, among others, demonstrated[7,8,19,29] that they could also provide a more accurate description of water dynamics than full charge models. While previous studies had mostly focused on cation parameters,[25–28] we have developed corresponding parameters for the halogen series in combination with the SPC/E water model.[7] Such an approach was subsequently repeated for the TIP4P-2005 water model, resulting in a large and comprehensive set of parameters for various ions that was published after this work was performed.[30,31]

Here we combine both DFT-based and ECC molecular dynamics simulations. While DFT-based simulations offer an explicit description of potential charge transfers in the solution, their substantial computational costs imposes strong limitations on the accessible simulation times; structural features are thus accessible with this technique but dynamical properties suffer from important uncertainties.[32] We therefore performed DFT-based simulations to determine the structure of the ionic aqueous solution and to validate the description obtained with the ECC classical simulations, which are then used to converge dynamical properties from long trajectories.

Simulation details

DFT-based molecular dynamics

DFT-based molecular dynamics simulations were performed on a solution consisting of a single Cs^+ ion and 117 water molecules placed in a 1.5295 nm-side cubic simulation box. The size of the box was determined from auxiliary classical molecular dynamics simulations at 1 atm. Born-Oppenheimer molecular dynamics simulations were performed with a time step of 0.5 fs using the Quickstep module[33] of the CP2K package (version 2.4) implementing the hybrid Gaussian functions and plane waves (GPW) method.[34] The system was at first equilibrated for 20 ps in the NVT ensemble employing the CSVR thermostat[35] with a time constant of 20 fs to target a temperature of 300 K. Two snapshots around 10 and 20 ps with total energy close to the average value were taken and propagated for 50 ps in the NVE en-

semble. The electronic structure of the system was treated at the DFT level with the revPBE functional[36] and the Grimme correction scheme (DFT-D2[37]) to account for dispersion interactions. The core electrons were described by norm-conserving GTH pseudopotentials.[38] Kohn-Sham orbitals were expanded in a DZVP MOLOPT Gaussian basis set.[34] A cutoff of 400 Ry was used for the auxiliary plane wave basis set.

Classical molecular dynamics

Classical molecular dynamics simulations were performed on a dilute aqueous solution containing a single cation (respectively Cs^+, Li^+ and Mg^{2+}) solvated by 513 water molecules. Force fields including electronic continuum correction were employed for the cations (respectively based on refs. 19,39 for Cs^+, ref. 27 for Li^+, and OPLS for Mg^{2+}) and all parameters are reported in Table 1. Water molecules were described by the TIP4P/2005 potential.[40]

Table 1: Cation force field parameters: Lennard-Jones potential radius and energy and atomic charge.

	σ (nm)	ϵ (kJ/mol)	q (e)
Cs^+	0.344	2.097	0.75
Li^+	0.18	0.07648	0.75
Mg^{2+}	0.16447	3.66118	1.50

Classical molecular dynamics simulations with a 2 fs time step were performed with the Gromacs-4.6.1 program package.[41] Each system was first equilibrated for 200 ps at 300 K and 1 bar, then the average box size was used for propagation in the NVT ensemble for 2 ns. The temperature was maintained by the CSVR thermostat[35] with a coupling constant of 0.1 ps, pressure was maintained at 1 bar by the Berendsen barostat[42] with a coupling constant of 0.5 ps. The bonds containing hydrogen atoms were constrained by the LINCS algorithm. Three-dimensional periodic boundary conditions were used. Short-range electrostatic and van der Waals interactions were truncated at 1.2 nm and long-range electrostatic interactions were treated via the particle mesh Ewald method[43] (the cation charge was neutralized with a diffuse negatively charged background). For the Cs^+ solutions, the same procedure was

repeated at 250 K, 275 K, 325 K and 350 K.

Comparison between DFT-based and ECC simulations

As already mentioned, typical classical forcefields fail to reproduce accelerated dynamics,[19–21] and always lead to retardations. While slower water dynamics is expected for Li^+ and Mg^{2+}, for which we therefore did not perform computationally expensive ab initio MD simulations, we verified that classical, non-polarizable ECC simulations could successfully reproduce the structure (and subsequently, the dynamics) of water around Cs^+ at 300 K, using an ab-initio trajectory as a reference.

In Fig. 1a, we compare the Cs^+–oxygen and Cs^+–hydrogen radial distribution functions for both types of simulations. The computed water structures around the cation are very similar. In particular, the peak positions and amplitudes are very well reproduced by the ECC approach. While small differences are present, they are negligible compared to the very large changes observed when the cation is changed in solutions of Li^+ and Mg^{2+} (obtained with ECC forcefields), which result in much sharper peaks and smaller hydration shells (Fig. 1b and c). This demonstrates that an ECC approach is successful in reproducing the solvation structure around Cs^+.

We then examine the reorientation dynamics. The slight acceleration of the OH reorientation dynamics in the hydration shell of Cs^+ is observed both for the aiMD and ECC simulations (Fig. 2a and b). Because of the high computational cost of the DFT-based setup, the fluctuations of the time-correlation function (tcf) are very large when we consider independent 10-ps portions of the 50-ps trajectory (Fig. 2a). While in most cases, the OH tcf in the shell decays slightly faster as compared to the bulk reference from the same block (averages at 300 K: 3.4 ps in the bulk vs 3.3 ps in the shell), they both suffer from large uncertainties, leading to considerable error bars (Fig. 2b) that preclude any quantitative discussion of the cations' effect on water dynamics. The much longer ECC simulations allow to obtain more converged OH tcfs (Fig. 2b), which can very well reproduce the slight

acceleration of dynamics in cesium's hydration shell (see main text for a more thorough discussion). This suggests that in contrast to prior suggestions,[21] ab initio MD simulations are not required to reproduce the acceleration of water dynamics next to some cations. We therefore used classical scaled-charge simulations whose affordable computational cost gives access to the long trajectories required to converge the solution dynamical properties.

Results and discussion

Prior experimental results on water dynamics in cations' hydration shells

The microscopic dynamics of water molecules in ionic aqueous solutions can be accessed by a number of experimental techniques. Different NMR strategies provide information regarding the water diffusion coefficient[44] and the reorientation time of water molecular vectors.[5,45–48] Ultrafast infrared (IR) spectroscopy directly probes the time-resolved reorientation of the OH groups.[4,49] THz ultrafast spectroscopy,[6,50] dielectric relaxation[51] and optical Kerr effect measurements[52] are sensitive to the dynamics of more collective modes of water reorganization dynamics. These experiments are necessarily performed on neutral salt solutions containing both anions and cations. A particular experimental difficulty arises from the signal being collected from all water molecules in the solution, whether in the ions' hydration shell or further away. Experiments thus employ solutions at a concentration that typically cannot go below a certain threshold depending on the sensitivity of the experimental setup. For example, ultrafast IR spectroscopy typically requires concentrated solutions to highlight effects that exceed experimental uncertainties. Isolating and understanding an ion's effect on water dynamics is thus not straightforward,[7] for several reasons: in a given solution, the anion and the cation both affect water dynamics, not necessarily to the same extent;[7] when increasing concentration, a viscosity increase[3] perturbs water dynamics independently of the effect of an isolated ion;[7] at high concentrations, ion-ion interactions become impor-

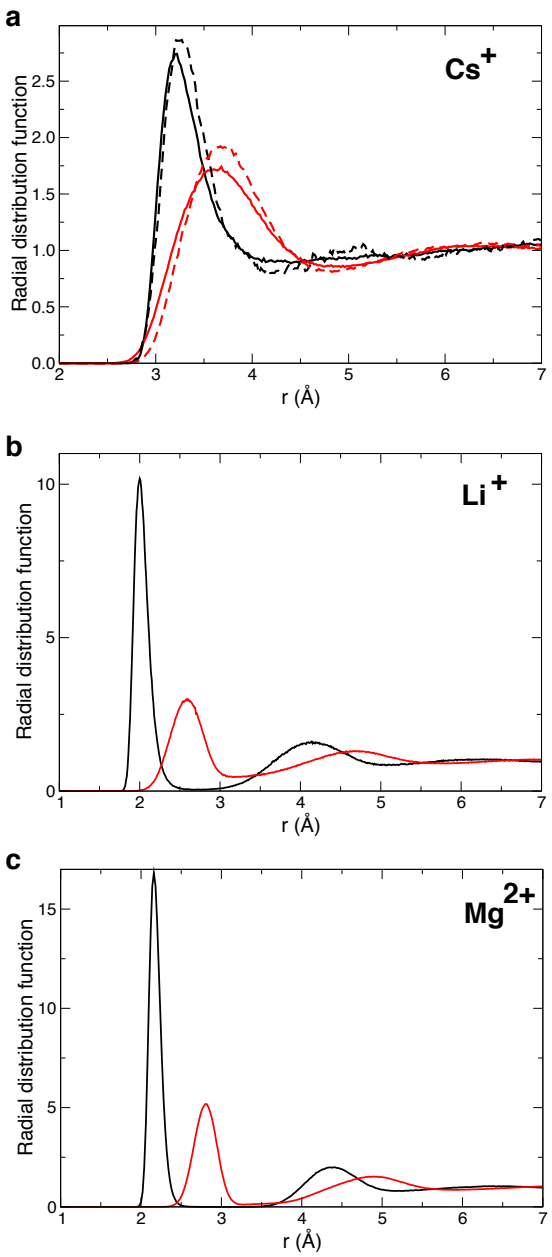

Figure 1: a) Radial distribution function between Cs^+ and the water oxygen (black) and hydrogen (red) atoms, respectively from the ECC (solid lines) and DFT-based (dashes) simulations b) Idem around Li^+ and c) around Mg^+ from ECC simulations.

tant, leading for example to different types of cation-anion ion pairs and to specific effects on water dynamics.[8,53]

Systematic NMR studies performed in the dilute regime (typically < 1 mol/L) for series of cations or anions in combination with a given counterion have quantified the amplitude

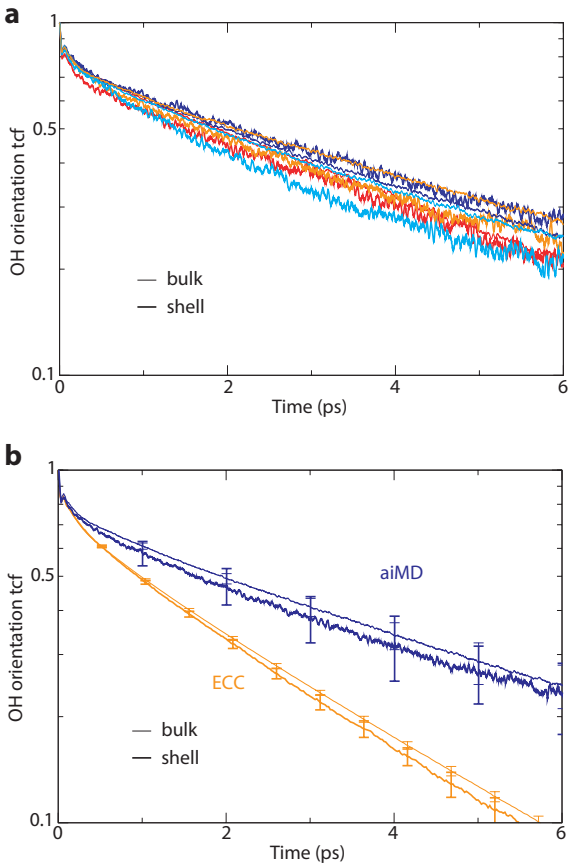

Figure 2: a) OH orientation tcf (Eq. 1) for bulk (thin lines) and hydration shell (thick lines) water molecules for the aiMD trajectory of Cs^+. Data was divided into 4 blocks of 25 ps each, shown by different colors. b) OH orientation tcf (Eq. 1) for bulk (thin lines) and hydration shell (thick lines) water molecules from the DFT-based trajectory (blue) and the ECC classical MD trajectory (orange). The error bars correspond to the 95% CI.

of the acceleration or retardation of water translational and reorientational dynamics due to isolated ions.[5,44,47,48] In dilute conditions, it was shown that the effect of a salt on water dynamics is well described by the sum of the effects caused by the anion and by the cation considered independently. For the series of alkaline cations, these measurements showed that Li^+ tends to significantly retard water dynamics, K^+ has barely any effect, and Cs^+ unambiguously leads to an acceleration. A similar trend is observed for anions, such as the halide series. These measurements are averaged over all water molecules in the system, and determining the effect of an ion on each water neighbor requires making assumptions regarding the size of the hydration shell and the lengthscale of the dynamical perturbations.[1]

These assumptions are supported by simulations which have demonstrated that for singly charged ions, the ion's effect on water reorientation dynamics is typically restricted to the first hydration shell,[7,8] whose size is directly determined from the simulations.

While the acceleration of water dynamics by Cs^+ has been unambiguously characterized using NMR, for both translational and reorientational motions, ultrafast IR spectroscopy measurements typically measured mild slowdowns for solutions containing Cs^+,[2] probably because it was then used in combination with anions such as sulfate that strongly retard water dynamics,[5] and at relatively high concentrations, where viscosity[7] and ion-pair effects[8] play a role. We note however that recent time-resolved two-dimensional Raman-THz measurements,[6] sensitive to more collective modes of water reorientation dynamics, were able to clearly report faster dynamics in Cs^+ solutions than in the bulk, contrasting with the slower dynamics observed with the same technique for aqueous solutions of other alkaline cations.

Simulated water reorientation times in cationic hydration shells

We first establish that the ECC MD simulations can successfully reproduce the acceleration of water dynamics by dilute Cs^+ cations and the slowdown induced by Li^+ and Mg^{2+} cations that have been reported by experiments. Because the different experimental techniques that have been employed to characterize water reorientation dynamics in ionic aqueous solutions probe different molecular vectors, we have computed the reorientation time-correlation function (tcf) relevant to each of them, defined as

$$C_{uu}(t) = \langle P_2 \left[\mathbf{u}(0) \cdot \mathbf{u}(t) \right] \rangle \tag{1}$$

where P_2 is the second-order Legendre polynomial and $\mathbf{u}(t)$ is the orientation of the molecular vector $\mathbf{u}$ at time t. We have considered the OH, HH and molecular dipole vectors and we have calculated the tcfs for water molecules which are in the cation first hydration shell (whose boundary is defined by the first minimum in the cation-oxygen radial distribution function,

see Fig. 1) at t=0, and for water molecules which are initially in a bulk-like environment far from the cation. Table 2 reports the reorientation relaxation times, defined as the time integrals of the tcf (Eq. 1), and their ratio with the bulk value, together with experimental data.[5]

The tcfs in Fig. 3 clearly show that our simulations successfully describe the acceleration of water reorientation dynamics in the Cs^+ hydration shell relative to the bulk, and the slower dynamics in the Li^+ and Mg^{2+} hydration shells. However, while the experimental trend is correctly reproduced, this agreement remains qualitative. As shown in Table 2, for the HH reorientation time which is measured by NMR spectroscopy,[5] the acceleration reported experimentally is underestimated by our simulations. This has been observed previously for other systems,[7,19,20] and scaled-charge approaches were found to systematically underestimate the experimental accelerations. DFT-based MD on a 3 M CsI solution[21] suffered from the same limitations, with reported translational dynamics only 8% faster than in bulk, as compared to more than 20% in the experiments.

Although mild, the acceleration caused by Cs^+ can be contrasted with the strong retardation of water reorientation dynamics in the hydration shell of cations with a higher charge density, such as Li^+ and Mg^{2+}. For the latter cations, our simulations reproduce the much slower dynamics observed in the experiments, but again underestimate the effect reported by the experiments. The trend observed in the simulations for the OH reorientation among Cs^+, Li^+ and Mg^{2+} is also consistent with time-resolved ultrafast IR spectroscopy measurements: for example, water reorientation dynamics in dilute 1 m solutions of Cs_2SO_4 and LiI is bulk-like.[2] These results are consistent with NMR predictions:[5] the SO_4^{2-} anion and the Li^+ cation both strongly retard water reorientation dynamics, while I^- and Cs^+ both induce accelerations. Therefore, a salt combining ions with antagonistic effects has, on average, no clear net effect on water dynamics. When combining two ions that perturb dynamics in the same way (for example, Mg^{2+} and SO_4^{2-}), water dynamics is indeed strongly affected, even in the dilute regime.[8]

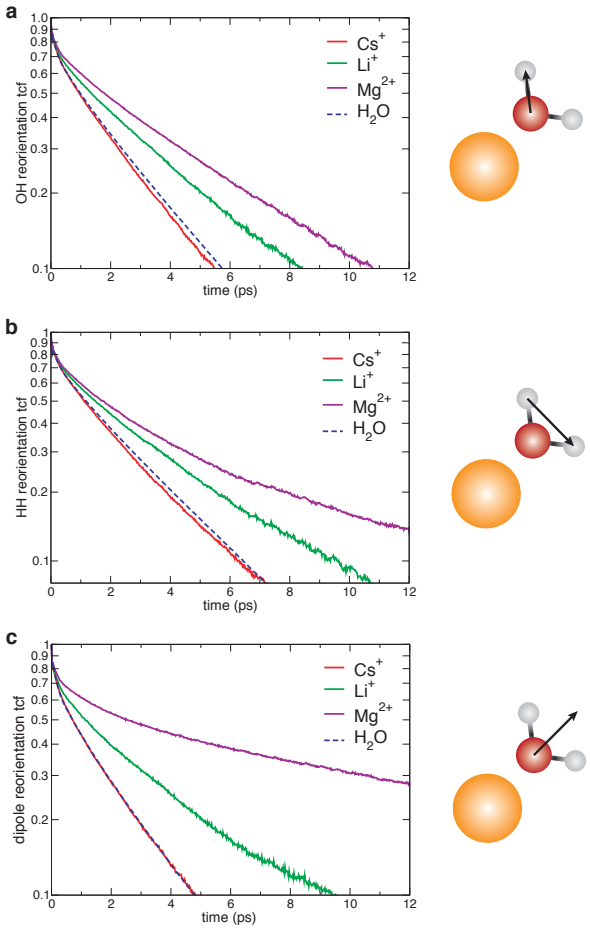

Figure 3: Water reorientation time correlation functions (Eq. 1) for water molecules initially in the Cs^+ (red), Li^+ (green) and Mg^{2+} (purple) hydration shells, and in the bulk (blue dashes), for a) the OH vector, b) the HH vector and c) the molecular dipole.

These results thus validate our approach and the employed molecular models. Before turning to a molecular interpretation of the retardation and acceleration of water dynamics by cations, we pause to analyze the anisotropy of water reorientation in cationic hydration shells.

Water reorientation anisotropy

Water reorientation in the bulk is slightly anisotropic, as already established by NMR spectroscopy and MD simulations,[54] and shown in our present simulations by the small differences in the reorientation time scales of the different molecular vectors (see Table 2). We now ex-

Table 2: Water dynamics in cationic hydration shells and in the bulk.

		bulk	Cs^+	Li^+	Mg^{2+}
HH reorientation	time (ps)	2.5	2.4	3.9	7.8
(Eq. 1)	shell/bulk ratio (exp. value[5])	1	0.98 (0.7)	1.6 (2.9)	3.2 (5.2)
OH reorientation	time (ps)	2.2	2.1	3.4	4.3
(Eq. 1)	shell/bulk ratio	1	0.97	1.6	2.0
dipole reorientation	time (ps)	1.8	1.8	4.1	14.6
(Eq. 1)	shell/bulk ratio	1	1.0	2.3	8.2
residence (Eq. 2)	time (ps)	-	3.6	58	> ns
H-bond jump	time (ps)	3.6	3.4	4.2	5.2
(Eq. 3)	retardation	1	0.95	1.2	1.5
frame reorientation	time (ps)	7.6	7.4	12.8	14.1
(Eq. 1)	retardation	1	0.97	1.7	1.9

amine whether cations enhance this reorientation anisotropy for the water molecules in their hydration shell. For example, it has been argued that cations would lock the dipoles of neighboring water molecules, leading to a "propeller"-like motion of the OH groups around the dipole axis.[2] As we will now see, densely-charged cations enhance the anisotropy of reorientational motions in their first hydration shell but the "locking" picture is oversimplified.

We first consider the reorientation tcfs in Fig. 3 and associated reorientation times in Table 2 for the water OH, HH and dipole vectors in the hydration shells of cations. For all investigated cations, the reorientation times of these molecular directions are different, which shows the presence of an anisotropy. Our results show that this anisotropy increases with the cation charge density. For Cs^+, the water reorientation anisotropy is very close to that in bulk water, without any significant enhancement by this cation, and the reorientation of the water dipole is faster than that of the OH and HH vectors. In contrast, for the Li^+ and Mg^{2+} cations, the reorientation of the water dipole is more retarded than that of the OH and HH vectors, and the anisotropy is much more pronounced. However, even next to Mg^{2+} the water dipole reorients on a picosecond timescale (The trend found here among the three investigated cations suggests that for cations with intermediate charge densities (e.g. K^+), water reorientation should be very close to isotropic.)

These results suggest that cations have a larger impact on the reorientation of water dipoles than on other water molecular axes. Figure 4 shows the probability density distribution for the angle between the cation–water oxygen direction and the water dipole orientation. It shows that cations with increasing charge density lead to a narrower angular distribution for the dipole orientations of water molecules in their hydration shell. However, it also reveals that even for cations with a high charge density the orientation of the surrounding water dipoles still displays considerable fluctuations around the cation–water oxygen direction.

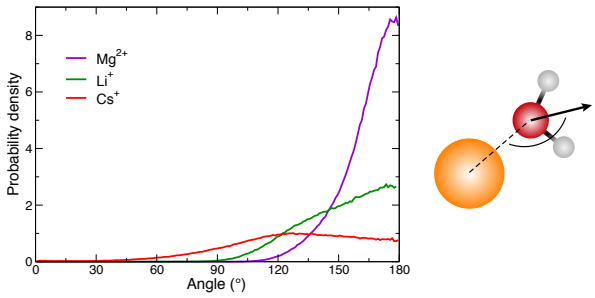

Figure 4: Probability density for the angle between cation–water oxygen direction and the water dipole orientation for the water molecules lying in the first hydration shell of Cs^+ (red), Li^+ (green) and Mg^{2+} (magenta), with the angle defined to be zero when the water dipole points toward the cation.

Two possible pathways could be considered for the reorientation of water dipoles next to cations: either via the departure of the water molecule from the first hydration layer, or via the reorientation of the cation–oxygen axis while the water molecule remains in the cation hydration shell. To discriminate between these two mechanisms, we calculated the water residence time in the cation hydration shell, defined as[55]

$$\tau_{res} = \int_0^\infty \mathrm{d}t \left[1 - \langle p_1(0) p_2(t) \rangle\right] \tag{2}$$

where $p_1(t)$ (resp. $p_2(t)$) is 1 for a water molecule which lies in the cation first (resp. second) hydration shell and 0 otherwise, with absorbing boundary conditions in the second shell. In the case of Li^+ and Mg^{2+}, our calculated residence time for water in the cation hydration shell

reported in Table 2 is at least one order of magnitude longer than the dipole reorientation time, which unambiguously shows that dipole reorientation mostly occurs while the molecule remains in the shell. Further support to this picture is provided by the cation–oxygen reorientation tcf whose long-time decay closely follows that of the dipole reorientation tcf (Figs. 3 and 5). It thus suggests that the water molecules remaining in the cation first hydration layer move on a picosecond timescale on a sphere corresponding to this hydration shell.

We also observe that for all three cations, the HH tcf decays to zero at long timescales. If reorientation were to occur on a cone around the dipole axis, at long delays the HH orientations would be uniformly distributed in the plane orthogonal to the cation–oxygen atom direction, so that $\langle[\mathbf{u}_{HH}(0) \cdot \mathbf{u}_{HH}(t)]^2\rangle = 1/2$ and the tcf (Eq. 1) would be expected to reach a $1/4$ plateau value, which is not seen in Fig. 3.

Our results thus demonstrate that a propeller-like reorientation picture[2] is oversimplified and largely exaggerated for hard cations like Li^+ and Mg^{2+} where the water dipole still reorients on a short timescale, and inadequate for soft cations like Cs^+ which do not cause a significant anisotropy in the surrounding water dynamics. We now focus on the molecular interpretation for the slowdown and acceleration of water OH reorientation dynamics in cationic hydration shells that was shown in experiments and in our simulations (Table 2).

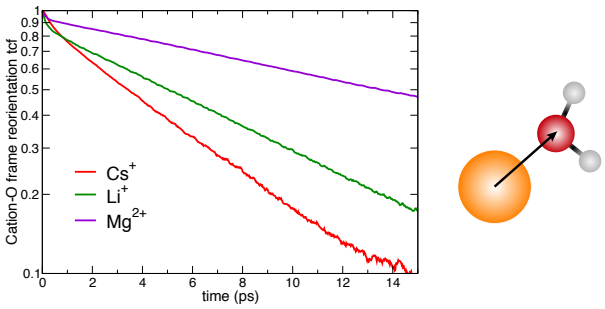

Figure 5: Reorientation tcf of the cation–oxygen vector for water molecules that initially lie in the cation first hydration shell (Cs^+ (red), Li^+ (green) and Mg^{2+} (magenta)).

Water reorientation mechanisms

Previous works on neat water and on a broad gamut of aqueous systems,[7,8,10,12–15,17,32,56–63] including ionic salt solutions,[7,8,14,15,64] have established that the picosecond-timescale water reorientation proceeds via two possible mechanisms. The dominant pathway occurs when one of the water OH groups exchanges H-bond acceptors, causing a large and sudden angular jump between the initial and final H-bond acceptors.[10] The presence of these angular jumps was first suggested based on molecular dynamics simulations and subsequently supported by nonlinear vibrational spectroscopy experiments in ionic aqueous solutions.[65,66] An additional, minor reorientation pathway arises from the diffusive reorientation of the intact H-bond axis between two consecutive jumps,[10] which corresponds to the slow tumbling of the local frame. Because jumps usually bring the major contribution to the overall OH reorientation time, including in the vast majority of aqueous solutions and interfaces that have been considered in previous work, any effect of a given solute or interface on water reorientation is usually to be understood in terms of its effect on the jump (or HB exchange) time.

In prior simulations studies of water dynamics in aqueous salt solutions, we have shown that the ion-induced acceleration and slowdown of water reorientation dynamics can be caused by the combination of three effects.[7,8,14,15,64] The first two are the result of the ions' effect on the H-bond exchange rate constant. Like other solutes, ions create a local excluded volume which hinders the approach for a new H-bond acceptor[56] and leads to a retardation of the H-bond exchange rate, and thus an increase in the reorientation time. Second, anions that can act as H-bond acceptors present an additional contribution due to the free energy cost to partially elongate the initial anion–water H-bond to reach the transition state for the exchange.[17,57] A third effect finally stems from changes in the solution viscosity in the presence of ions, which typically lead to a retardation of the diffusive frame reorientation.[7] This contribution becomes more prominent at higher concentrations, where viscosity can be greatly increased,[7] which explains why even salts that accelerate water dynamics in the dilute regime tend to retard water reorientation at high concentrations.[5]

We first determine the jump and frame reorientation components of the extended jump model[10] for the reorientation of water molecules within cationic hydration shells. The H-bond jump time for a water OH group between H-bond acceptors is calculated as

$$\tau_j = \int_0^\infty \mathrm{d}t \; C_j(t) \tag{3}$$

where the jump tcf is

$$C_j(t) = [1 - \langle p_i(0) p_f(t) \rangle] \tag{4}$$

$p_i(t)$ (resp. $p_f(t)$) is 1 when the water OH group is H-bonded to its initial (resp. final) H-bond acceptor, using stable H-bond geometric criteria and absorbing boundary conditions in the final state (see ref. 11 for details). The jump tcfs are shown in Fig. 6. In contrast to H-bond exchanges in anionic shells which involve the anion as H-bond acceptor, exchanges in cationic shells take place between two water H-bond acceptors. The frame reorientation due to intact H-bond tumbling is calculated from the reorientation tcf of the H-bond O–O axis between successive H-bond jumps. The results in Table 2 show that as in the case of anion hydration shells, H-bond jumps remain the main reorientation pathway for water molecules next to cations. H-bond exchanges are slightly faster next to Cs^+ than in the bulk, while they are retarded next to Li^+ and most notably next to Mg^{2+}. Our results show that even if the reorientation dynamics of the different water molecular axes and H-bond dynamics are not affected to the same extent by cations, the trend is the same for all these timescales when one compares the respective impacts of Cs^+, Li^+ and Mg^{2+}, with an acceleration relative to the bulk for Cs^+ and an increasing slowdown for Li^+ and Mg^{2+}. We therefore now focus on the effect of cations on the H-bond jump time in order to elucidate its molecular origin.

Contributions to H-bond jump free energy barrier

Prior work[11] has established that the free energy barrier to reach the jump transition state configuration is essentially due to the free energy costs for the elongation of the initial H-

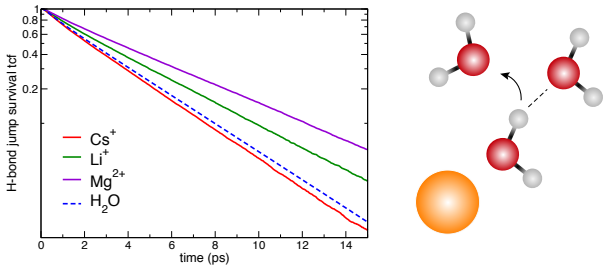

Figure 6: H-bond jump tcf (Eq. 4) for a water molecule initially in the cation hydration shell, Cs^+ (red), Li^+ (green) and Mg^{2+} (purple) hydration shells, and in the bulk (blue dashes).

bond and for the approach of the new H-bond acceptor. It has been shown[67] that the jump free energy barrier can be approximated by the sum of these two independent contributions

$$\Delta G^{\ddagger}_{\text{jump}} \simeq \Delta G^{\ddagger}_{\text{elongation}} + \Delta G^{\ddagger}_{\text{approach}}. \tag{5}$$

We start with the free energy cost for the approach of a new H-bond partner $\Delta G^{\ddagger}_{\text{approach}}$. Our extensive prior work[12] on the effect of solutes on water H-bond dynamics has shown that all solutes contribute to an increase in $\Delta G^{\ddagger}_{\text{approach}}$ through a transition state excluded volume (TSEV) effect:[56] the solute hinders the approach of a potential new acceptor, reduces the number of accessible transition state configurations for the new H-bond partner, and thus increases the entropic barrier. This TSEV effect induces a slowdown with respect to the bulk dynamics, which was determined in prior simulations by calculating the fraction of jump transition-state geometries that would be accessible in the bulk but that are blocked by the solute.[56] The TSEV effect was shown[56] to be the origin of the slowdown in water H-bond dynamics in the hydration shell of hydrophobic solutes and to have an important effect on water dynamics for all solutes including, e.g. proteins.[12] Notably, it explains why isolated (and typically convex) solutes lead to a retardation of H-bond exchange dynamics that is below 2,[56,68] and why concentrated solutions, where solvation shells overlap, can lead to stronger retardation,[69] with excluded volume contribution now exceeding half of the transition state geometries.

Solutes can also affect the free energy cost to elongate the initial H-bond in order to reach the jump transition state geometry $\Delta G^{\ddagger}_{\text{elongation}}$. This transition state hydrogen bond (TSHB) strength effect was shown[17,59] to be particularly important for solutes which accept an H-bond from water, including, e.g., anions. For solutes whose H-bonds with water are stronger than water–water H-bonds, the TSHB effect increases the jump free energy barrier and thus induces a slowdown, and vice-versa for solutes which accept weak H-bonds from water. The TSHB effect explains why isolated H-bond acceptors give rise to a retardation factor than can exceed a factor of 2 as compared to bulk, when they form very strong H-bond with water, or, accelerations, when these H-bonds are much weaker than in the bulk.[17]

Hydration structure and ion-excluded volume

We now determine the cationic excluded volumes from the structures of the ion hydration shells. In the bulk, the $\Delta G^{\ddagger}_{\text{approach}}$ and $\Delta G^{\ddagger}_{\text{elongation}}$ free energies can be determined from the water oxygen–oxygen radial distribution function.[67] In the vicinity of cations, the bulk radial symmetry is broken. We therefore focus on water molecules lying within the cation first hydration shell and determine the probability $p\,(R_{O_sO}, \theta_{OO_sX})$ to find a water oxygen atom at distance R_{O_sO} from the shell oxygen O_s and at an angle θ_{OO_sX} with respect to the O_sX shell oxygen–cation direction (see scheme in Fig. 7).

Figure 7 shows these probability distributions for the Cs^+, Li^+ and Mg^{2+} cations. In agreement with the dipole orientations reported in Fig. 4, these plots reveal that first shell water molecules donate H-bonds to oxygen atoms lying further away from the cation, leading to a peak at $R_{O_sO} \simeq 2.8$ Å and $\theta_{OO_sX} > 90°$. For all ions, an excluded volume region is visible at short R_{O_sO} distances and small θ_{OO_sX} angle (i.e. in the direction of the cation). In the hydration shells of Li^+ and Mg^{2+}, additional peaks at $R_{O_sO} \simeq$3–5Å and $\theta_{OO_sX} < 90°$ are visible and correspond to other water molecules lying in the cation first shell. However, the vanishing probability between these additional peaks and the H-bond acceptor peak ($\theta_{OO_sX} > 90°$) shows that no H-bond exchange is possible with these other first shell

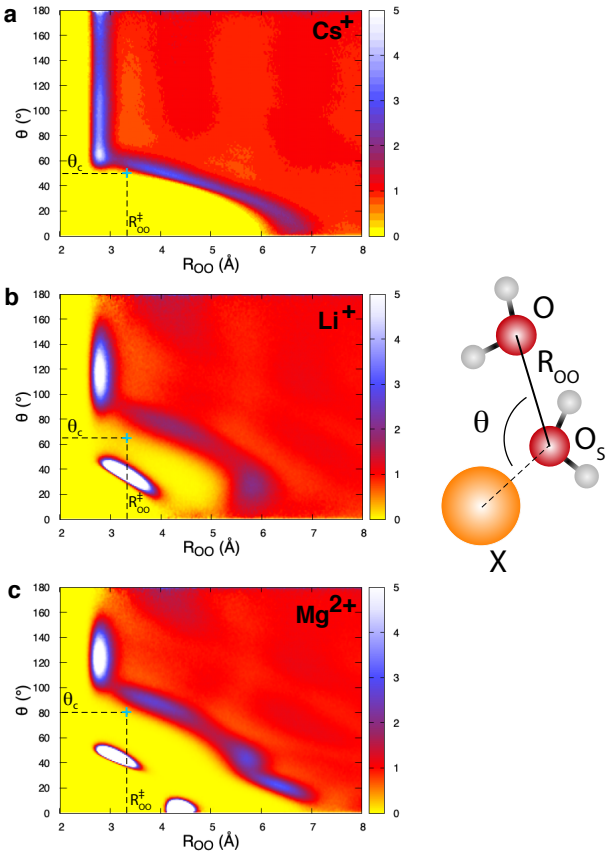

Figure 7: Probability distribution $p\,(R_{O_sO}, \theta_{OO_sX})$ to find a water oxygen at distance R_{O_sO} (simplified into R_{OO} in the axis label) from a shell oxygen O_s and at an angle θ_{OO_sX} (simplified into θ in the axis label) with respect to the O_sX shell oxygen–cation direction for a) Cs^+, b) Li^+ and c) Mg^{2+}. The θ_{OO_sX} used for the definition of the excluded volume fraction (Eq. 6 and Eq. 9) corresponds to the position where the probability vanishes (blue cross) at the transition state OO distance $R^{\ddagger}_{OO}$. Probabilities were normalized to reach 1 for large R_{O_sO} separations.

molecules, which should therefore be excluded from the list of potential new acceptors, as now detailed. We approximate the excluded volume at distance O_sO from a shell oxygen O_s by determining the θ_{OO_sX} angle when the water oxygen O is at the minimum approach distance R_c from the cation X (Fig. 8). Simple geometric considerations yield

$$\theta_{OO_sX} = \left(OO_s^2 + XO_s^2 - R_c^2\right) / \left(2\ OO_s\ XO_s\right) \tag{6}$$

The R_c and XO_s parameters are fitted from the distributions in Fig. 7 and we obtain

R_c=2.75 Å, CsO=3.2 Å for Cs^+, R_c=3.0 Å, LiO=2.5 Å for Li^+ and R_c=3.7 Å, MgO=2.3 Å for Mg^{2+}.

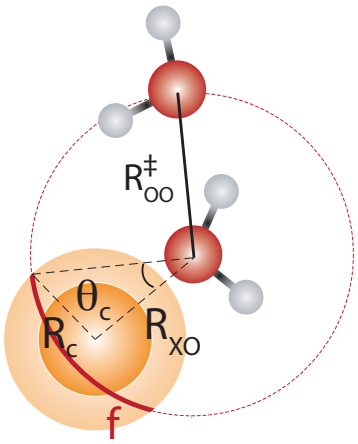

Figure 8: Geometric definition of the excluded volume fraction f (Eq. 6 and Eq. 9).

The free energy cost to elongate the initial H-bond donated by a water molecule lying in the cation shell is determined from the potential of mean force w_{OO} along the OO distance,[67] obtained from the OO radial distribution function g_{OO}^{corr} corrected for the excluded volume identified in the probability distribution (Fig. 7):

$$\Delta G^{\ddagger}_{\text{elongation}} = w_{OO}(R^{\ddagger}_{OO}) - w_{OO}(R^{eq}_{OO}) = -k_B T \ln \left[\frac{g^{corr}_{OO}(R^{\ddagger}_{OO})}{g^{corr}_{OO}(R^{eq}_{OO})} \right] \tag{7}$$

where R^{eq}_{OO} is the OO_s distance of the first peak in the radial distribution function, and $R^{\ddagger}_{OO}$ is the OO_s distance at the jump transition state, which we approximate by the distance at the first minimum in the radial distribution function. The change with respect to the bulk is thus

$$\Delta\Delta G^{\ddagger}_{\text{elongation}} = \Delta G^{\ddagger shell}_{\text{elongation}} - \Delta G^{\ddagger bulk}_{\text{elongation}} = -k_B T \ln \left[\frac{g^{corr}_{OO}(R^{\ddagger}_{OO})}{g^{corr}_{OO}(R^{eq}_{OO})} \frac{g^{bulk}_{OO}(R^{eq}_{OO})}{g^{bulk}_{OO}(R^{\ddagger}_{OO})} \right] \tag{8}$$

The corrected radial distribution function and associated potential of mean force in Fig. 9 reveal that the presence of the cation reduces the strength of the surrounding water–water H-bonds and decreases the free energy barrier $\Delta G^{\ddagger}_{\text{elongation}}$ to elongate them and reach the

H-bond jump transition state. This effect is particularly pronounced in the hydration layer of Cs^+ ($\Delta G^{\ddagger}_{\text{elongation}}$ $\simeq$0.85 kcal/mol in the bulk, 0.77 kcal/mol next to Cs^+ and 0.80 kcal/mol next to Li^+ and Mg^{2+}). Quite surprisingly, the presence of any of these three cations thus facilitates the initial H-bond elongation, and this contribution tends to accelerate the H-bond dynamics.

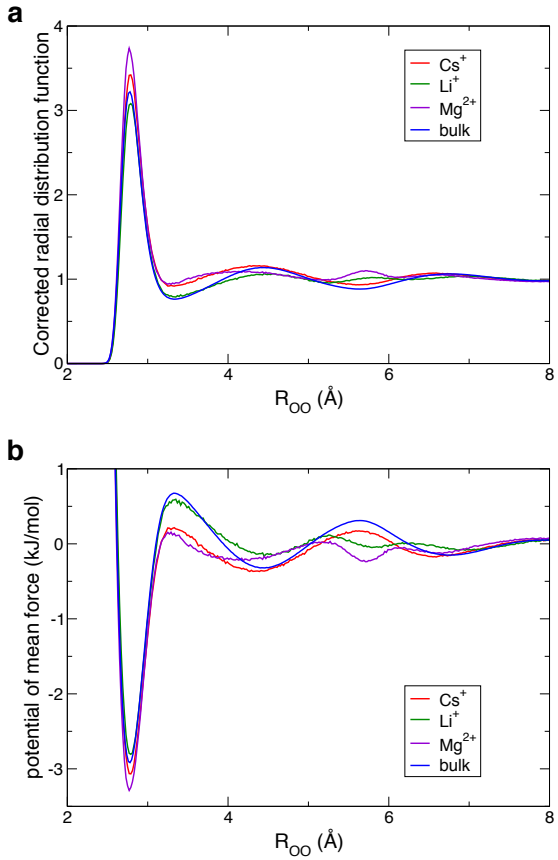

Figure 9: a) Oxygen–oxygen radial distribution function and b) potential of mean force around a water molecule lying in the cation first hydration shell and corrected for the cation excluded volume.

However, as we will now see, the cations differ by their effect on the new H-bond acceptor approach. To estimate the fraction of transition state configurations for the new acceptor that would be possible in the bulk but are inaccessible in the vicinity of the cation, we consider the sphere centered on a first shell water oxygen atom and whose radius is the $R^{\ddagger}_{OO}$ transition state distance. The fraction of this sphere excluded by the cation is $f = (1 - \cos\,\theta_c)/2$,

where θ_c is the θ_{OO_sX} angle in Eq. 6 determined at $R^{\ddagger}_{OO}$. The resulting (entropic) increase in $\Delta G^{\ddagger}_{\text{approach}}$ with respect to the bulk is[56]

$$\Delta\Delta G^{\ddagger}_{\text{approach}} = -k_B T \ln\left[\left(1+\cos\,\theta_c\right)/2\right] \tag{9}$$

The θ_c values determined from Fig. 7 are respectively $\simeq 50°$ for Cs^+, $\simeq 65°$ for Li^+ and $\simeq 80°$ for Mg^{2+}. We note that these excluded volume fractions do not follow the size of the cations that would be inferred from the first peak in the cation–oxygen radial distribution function Fig. 1. This is due to the effect of the cation "hardness". While Cs^+ is larger than Mg^{2+}, its softer character allows water molecules to move closer to the cation, as seen from the large width of the first peak in the cation–oxygen radial distribution function, while Mg^{2+} exhibits a more repulsive interaction with water.

The ratio of the water H-bond jump times in the cation shell and in the bulk is thus determined by the change in $\Delta\Delta G^{\ddagger}_{\text{elongation}}$ and $\Delta\Delta G^{\ddagger}_{\text{approach}}$ between bulk and ion shell and we combine the TSEV and TSHB factors (Eqs. 8,9) to yield,

$$\tau_j^{shell}/\tau_j^{bulk} = \exp\left[\frac{\Delta\Delta G^{\ddagger}_{\text{elongation}} + \Delta\Delta G^{\ddagger}_{\text{approach}}}{k_B T}\right] = \frac{2}{1+\cos\,\theta_c}\frac{g_{OO}^{bulk}(R^{\ddagger}_{OO})}{g_{OO}^{bulk}(R^{eq}_{OO})}\frac{g_{OO}^{corr}(R^{eq}_{OO})}{g_{OO}^{corr}(R^{\ddagger}_{OO})} \tag{10}$$

The results in Fig. 11 show that the model of Eq. 10 provides an excellent description of the change in the water H-bond jump time in the cation hydration shell when comparing Cs^+, Li^+ and Mg^{2+}. While the model slightly overestimates the ion-induced slowdown, it can successfully reproduce the faster water dynamics next to Cs^+ compared to Mg^{2+}.

A critical demonstration of the important role played by the TSHB factor in the overall acceleration/retardation is provided by the temperature dependence of the reorientation dynamics in the Cs^+ hydration shell. Experimentally, Cs^+ is known to accelerate water reorientation at ambient temperature, but becomes a slight retardant at 350 K.[5] Such temperature-dependence cannot result from the purely entropic TSEV contribution, which would predict a fixed retardation at all temperatures. In order to test our model, we repeated

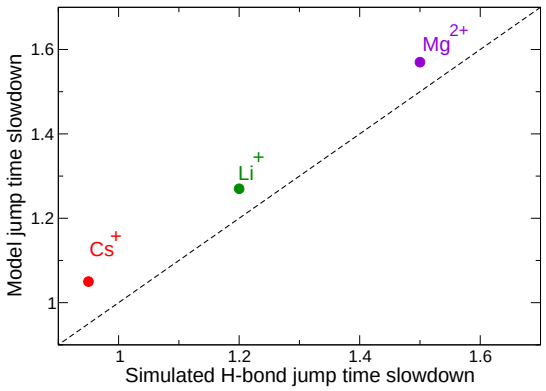

Figure 10: Correlation between the ratios of H-bond jump times in the cation hydration shell and in the bulk obtained directly from our simulations and from the combination of the excluded volume and H-bond strength factors (Eq. 10).

the calculations of the TSHB and TSEV contributions between 250 K and 350 K, using the same procedure by recalculating the corrected potentials of mean force at each intermediate temperature and taking the same excluded volume cone angle of 50° (which we verified to change very little with temperature).

In Fig. 11, we show that the combination of the TSEV and TSHB effects can successfully explain the temperature-dependence of the reorientation dynamics in the simulations, itself in agreement with experimental trends.[5] As temperature increases, the enthalpic destabilization contribution to the H-bond exchange time becomes less prominent, which eventually leads to a retardation at high temperatures. In contrast, when temperature decreases, it largely exceeds the entropic contribution to the TSHB effect and the TSEV effect, which leads to marked accelerations, as seen in our simulations and in the experiments (Fig. 11).

Conclusions

Ions lead to significant structural, dynamical and thermodynamical changes in water properties.[1,2,4–9] Building on a predictive framework that we developed over the years in order to rationalize the molecular origins of solute's and interface's effects on water reorientation dy-

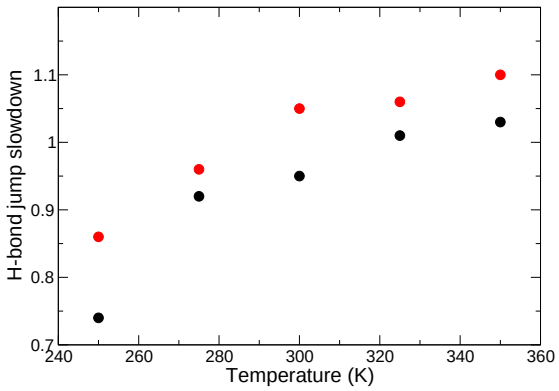

Figure 11: Temperature dependence of the H-bond jump time ratios between the Cs^+ cation hydration shell and the bulk obtained directly from our simulations (black) and from the combination of the excluded volume and H-bond strength factors eq. 10 (red).

namics,[7,8,10,12–15,17,32,56–63] we hereby provide a molecular understanding of why some cations accelerate water reorientation, why others retard it, and why these effects are temperature dependent.[5]

A first requirement for a successful approach based on classical molecular dynamics simulations is the use of a forcefield that is able to reproduce the experimental observations. Because typical non-polarizable forcefields fail to account for the accelerations measured next to some cations, it has been argued that only models that include explicit polarization, charge transfer, or even ab-initio MD, would be required to capture these effects. We first demonstrate that taking into account polarizability implicitly through charge rescaling allows to obtain results in qualitative agreement with the experiments, in line with previous suggestions.[7,8,19,29]

We then study the anisotropy of water reorientation in cationic hydration shells. While cations with a high charge density tend to strongly orient the water dipole, the OH reorientation is less affected. However, a picture where the dipole would be locked,[2] with free reorientation of the OH group, is not correct. For weak cations, such as Cs^+, reorientation of the dipole and of the OH groups is accelerated or almost bulk-like; for Li^+ and Mg^{2+}

that strongly bind water, reorientation of the dipole is possible through the tumbling the the cation–oxygen axis, which typically occurs on a picosecond timescale.

We then demonstrate that the framework provided by the extended jump model allows to understand the faster OH reorientation in the Cs^+ hydration shell at ambient temperature, and the slower reorientation in Li^+ and Mg^{2+} hydration shells. We demonstrate that a combination of two effects on the hydrogen-bond (H-bond) exchange dynamics allow to understand the ambient temperature acceleration of water reorientation next to Cs^+, and the retardation next to Li^+ and Mg^{2+}. First, ions create a local excluded volume, which hinders the approach of possible new H-bond partners, leading to a retarding contribution. However, they also perturb the local water structure, reducing the energetic cost to the initial H-bond elongation. For Cs^+ at room temperature, this latter contribution overcomes the excluded volume effect, leading to an acceleration. For Li^+ and Mg^{2+}, the excluded volume effect dominates, which leads to an overall retardation of the H-bond exchange. Moreover, the strong temperature-dependence observed in the experiments for Cs^+ (i.e., a large acceleration close to freezing and a retardation close to boiling) is understood by the key enthalpic effect of the elongation contribution.

While the combination of a transition-state excluded volume effect together with a distortion of the H-bond network allows to understand the effects of the three investigated cations, we note that the simplicity of the extended jump model approach involves a number of simplifications. In particular, for cations that strongly orient the water dipole, reorientation of the OH groups through H-bond exchanges is more constrained than in the bulk. As a consequence, H-bond exchanges are certainly not as isotropic as in the bulk, and the current extended jump model which assumes homogeneous, isotropic reorientation in three dimensions would need further extensions to account for this anisotropy.

Overall, our framework now allows to reach a comprehensive understanding of cations' and anions' effects on water reorientation dynamics. Our model not only offers a consistent interpretation of existing experimental and simulation results, but it can also help designing

ionic aqueous solutions with tailored dynamical properties, which have important consequences for phenomena including proton transfer, proton mobility, and chemical reactivity.

Acknowledgement

The research leading to these results has received funding from the European Research Council under the European Union's Seventh Framework Program (FP7/ 2007-2013)/ERC Grant Agreement No. 279977.

Data availability

The data that support the findings of this study are available from the corresponding authors upon reasonable request.

References

(1) Marcus, Y. Effect of ions on the structure of water: structure making and breaking. *Chem. Rev.* **2009**, *109*, 1346–1370.

(2) Tielrooij, K. J.; Garcia-Araez, N.; Bonn, M.; Bakker, H. J. Cooperativity in ion hydration. *Science* **2010**, *328*, 1006–1009.

(3) Donald, H.; Jenkins, B.; Marcus, Y. Viscosity S-coefficients of ions in solution. *Chem. Rev.* **1995**, *95*, 2695–2724.

(4) Bakker, H. J. Structural dynamics of aqueous salt solutions. **2008**, *108*, 1456–1473.

(5) Endom, L.; Hertz, H. G.; Thül, B.; Zeidler, M. D. A microdynamic model of electrolyte solutions as derived from nuclear magnetic relaxation and self-diffusion data. *Ber. Bunsenges. Phys. Chem.* **1967**, *71*, 1008–1228.

(6) Shalit, A.; Ahmed, S.; Savolainen, J.; Hamm, P. Terahertz echoes reveal the inhomogeneity of aqueous salt solutions. *Nat. Chem.* **2017**, *9*, 273–278.

(7) Laage, D.; Stirnemann, G. Effect of ions on water dynamics in dilute and concentrated aqueous salt solutions. *J. Phys. Chem. B* **2019**, *123*, 3312–3324.

(8) Stirnemann, G.; Wernersson, E.; Jungwirth, P.; Laage, D. Mechanisms of acceleration and retardation of water dynamics by ions. *J. Am. Chem. Soc.* **2013**, *135*, 11824–11831.

(9) Rinne, K. F.; Gekle, S.; Netz, R. R. Ion-specific solvation water dynamics: single water versus collective water effects. *J. Phys. Chem. A* **2014**, *118*, 11667–11677.

(10) Laage, D.; Hynes, J. T. A molecular jump mechanism of water reorientation. *Science* **2006**, *311*, 832–835.

(11) Laage, D.; T, H. J. On the molecular mechanism of water reorientation. *J. Phys. Chem. B* **2008**, *112*, 14230–14242.

(12) Laage, D.; Stirnemann, G.; Sterpone, F.; Rey, R.; Hynes, J. T. Reorientation and allied dynamics in water and aqueous solutions. *Annu. Rev. Phys. Chem.* **2011**, *62*, 395–416.

(13) Laage, D.; Stirnemann, G.; Sterpone, F.; Hynes, J. T. Water jump reorientation: from theoretical prediction to experimental observation. *Acc. Chem. Res.* **2012**, *45*, 53–62.

(14) Boisson, J.; Stirnemann, G.; Laage, D.; Hynes, J. T. Water reorientation dynamics in the first hydration shells of F- and I-. *Phys. Chem. Chem. Phys.* **2011**, *13*, 19895–19901.

(15) Stirnemann, G.; Jungwirth, P.; Laage, D. Water dynamics in concentrated electrolytes: local ion effect on hydrogen-bond jumps rather than collective coupling to ion clusters. *Proc. Natl. Acad. Sci. U.S.A.* **2018**, *115*, E4953–E4954.

(16) Roget, S. A.; Carter-Fenk, K. A.; Fayer, M. D. Water dynamics and structure of highly concentrated licl solutions investigated using ultrafast infrared spectroscopy. *J. Am. Chem. Soc.* **2022**, *144*, 4233–4243, PMID: 35226487.

(17) Sterpone, F.; Stirnemann, G.; Hynes, J. T.; Laage, D. Water hydrogen-bond dynamics around amino acids: the key role of hydrophilic hydrogen-bond acceptor groups. *J. Phys. Chem. B* **2010**, *114*, 2083–2089.

(18) Mancinelli, R.; Botti, A.; Bruni, F.; Ricci, M. A.; Soper, A. K. Hydration of sodium, potassium, and chloride ions in solution and the concept of structure maker/breaker. *J. Phys. Chem. B* **2007**, *111*, 13570–13577.

(19) Kann, Z. R.; Skinner, J. L. A scaled-ionic-charge simulation model that reproduces enhanced and suppressed water diffusion in aqueous salt solutions. *J. Chem. Phys.* **2014**, *141*, 104507.

(20) Kim, J. S.; Wu, Z.; Morrow, A. R.; Yethiraj, A.; Yethiraj, A. Self-diffusion and viscosity in electrolyte solutions. *J. Phys. Chem. B* **2012**, *116*, 12007–12013.

(21) Ding, Y.; Hassanali, A. A.; Parrinello, M. Anomalous water diffusion in salt solutions. *Proc. Natl. Acad. Sci. U.S.A.* **2014**, *111*, 3310–3315.

(22) Berkowitz, M. L. Molecular simulations of aqueous electrolytes: role of explicit inclusion of charge transfer into force fields. *J. Phys. Chem. B* **2021**, *125*, 13069–13076.

(23) Leontyev, I.; Stuchebrukhov, A. Accounting for electronic polarization in non-polarizable force fields. *Phys. Chem. Chem. Phys.* **2011**, *13*, 2613–2626.

(24) Duboué-Dijon, E.; Javanainen, M.; Delcroix, P.; Jungwirth, P.; Martinez-Seara, H. A practical guide to biologically relevant molecular simulations with charge scaling for electronic polarization. *J. Chem. Phys.* **2020**, *153*, 050901.

(25) Mason, P. E.; Wernersson, E.; Jungwirth, P. Accurate description of aqueous carbonate ions: an effective polarization model verified by neutron scattering. *J. Phys. Chem. B* **2012**, *116*, 8145–8153.

(26) Pluhařová, E.; Mason, P. E.; Jungwirth, P. Ion pairing in aqueous lithium salt solutions with monovalent and divalent counter-anions. *J. Phys. Chem. A* **2013**, *117*, 11766–11773.

(27) Pluhařová, E.; Fischer, H. E.; Mason, P. E.; Jungwirth, P. Hydration of the chloride ion in concentrated aqueous solutions using neutron scattering and molecular dynamics. *Mol. Phys.* **2014**, *112*, 1230–1240.

(28) Kohagen, M.; Mason, P. E.; Jungwirth, P. Accounting for electronic polarization effects in aqueous sodium chloride via molecular dynamics aided by neutron scattering. *J. Phys. Chem. B* **2016**, *120*, 1454–1460.

(29) Yue, S.; Panagiotopoulos, A. Z. Dynamic properties of aqueous electrolyte solutions from non-polarisable, polarisable, and scaled-charge models. *Mol. Phys.* **2019**, *117*, 3538–3549.

(30) Zeron, I. M.; Abascal, J. L.; Vega, C. A force field of Li^+, Na^+, K^+, Mg^{2+}, Ca^{2+}, Cl^-, and SO_4^{2-} in aqueous solution based on the TIP4P/2005 water model and scaled charges for the ions. *J. Chem. Phys.* **2019**, *151*, 044505.

(31) Blazquez, S.; Conde, M. M.; Abascal, J. L.; Vega, C. The Madrid-2019 force field for electrolytes in water using TIP4P/2005 and scaled charges: extension to the ions F^-, Br^-, I^-, Rb^+, and Cs^+. *J. Chem. Phys.* **2022**, *156*.

(32) Stirnemann, G.; Duboué-Dijon, E.; Laage, D. Ab initio simulations of water dynamics in aqueous TMAO solutions: temperature and concentration effects. *J. Phys. Chem. B* **2017**, *121*, 11189–11197.

(33) VandeVondele, J.; Krack, M.; Mohamed, F.; Parrinello, M.; Chassaing, T.; Hutter, J. QUICKSTEP: fast and accurate density functional calculations using a mixed gaussian and plane waves approach. *Comput. Phys. Commun.* **2005**, *167*, 103–128.

(34) VandeVondele, J.; Hutter, J. Gaussian basis sets for accurate calculations on molecular systems in gas and condensed phases. *J. Chem. Phys.* **2007**, *127*, 114105.

(35) Bussi, G.; Donadio, D.; Parrinello, M. Canonical sampling through velocity rescaling. *J. Chem. Phys.* **2007**, *126*, 014101.

(36) Zhang, Y.; Yang, W. Comment on "Generalized gradient approximation made simple". *Phys. Rev. Lett.* **1998**, *80*, 890–890.

(37) Grimme, S. Semiempirical gga-type density functional constructed with a long-range dispersion correction. *J. Comput. Chem.* **2006**, *27*, 1787–1799.

(38) Goedecker, S.; Teter, M.; Hutter, J. Separable dual-space Gaussian pseudopotentials. *Phys. Rev. B* **1996**, *54*, 1703–1710.

(39) Mao, A. H.; Pappu, R. V. Crystal lattice properties fully determine short-range interaction parameters for alkali and halide ions. *J. Chem. Phys.* **2012**, *137*, 064104.

(40) Abascal, J. L.; Vega, C. A general purpose model for the condensed phases of water: TIP4P/2005. *J. Chem. Phys.* **2005**, *123*, 234505.

(41) Hess, B.; Kutzner, C.; van der Spoel, D.; Lindahl, E. GROMACS 4: algorithms for highly efficient, load-balanced, and scalable molecular simulation. *J. Chem. Theo. Comput.* **2008**, *4*, 435–447, PMID: 26620784.

(42) Berendsen, H. J. C.; Postma, J. P. M.; van Gunsteren, W. F.; DiNola, A.; Haak, J. R. Molecular dynamics with coupling to an external bath. *J. Chem. Phys.* **1984**, *81*, 3684–3690.

(43) Essmann, U.; Perera, L.; Berkowitz, M. L.; Darden, T.; Lee, H.; Pedersen, L. G. A smooth particle mesh Ewald method. *J. Chem. Phys.* **1995**, *103*, 8577–8593.

(44) Müller, K. J.; Hertz, H. G. A parameter as an indicator for water-water association in solutions of strong electrolytes. *J. Phys. Chem.* **1996**, *100*, 1256–1265.

(45) Lang, E.; Lüdemann, H. D. Pressure and temperature dependence of the longitudinal proton relaxation times in supercooled water to -87 °C and 2500 bar. *J. Chem. Phys.* **1977**, *67*, 718–723.

(46) Jonas, J.; DeFries, T.; Wilbur, D. J. Molecular motions in compressed liquid water. *J. Chem. Phys.* **1976**, *65*, 582–588.

(47) Engel, G.; Hertz, H. On the negative hydration. A nuclear magnetic relaxation study. *Ber. Bunsenges. Phys. Chem.* **1968**, *72*, 808–834.

(48) Fister, B. F.; Hertz, H. G. O^{17}-NMR study of aqueous electrolyte and non-electrolyte solutions. *Ber. Bunsenges. Phys. Chem.* **1967**, 1032–1040.

(49) Bakker, H. J.; Skinner, J. L. Vibrational spectroscopy as a probe of structure and dynamics in liquid water. *Chem. Rev.* **2010**, *110*, 1498–1517.

(50) Heugen, U.; Schwaab, G.; Brundermann, E.; Heyden, M.; Yu, X.; Leitner, D. M.; Havenith, M. Solute-induced retardation of water dynamics probed directly by terahertz spectroscopy. *Proc. Natl. Acad. Sci. U.S.A.* **2006**, *103*, 12301–12306.

(51) Tielrooij, K. J.; Paparo, D.; Piatkowski, L.; Bakker, H. J.; Bonn, M. Dielectric relaxation dynamics of water in model membranes probed by Terahertz spectroscopy. *Biophys. J.* **2009**, *97*, 2484–2492.

(52) Winkler, K.; Lindner, J.; Bürsing, H.; Vöhringer, P. Ultrafast raman-induced kerr-effect of water: single molecule versus collective motions. *J. Chem. Phys.* **2000**, *113*, 4674–4682.

(53) Vila Verde, A.; Santer, M.; Lipowsky, R. Solvent-shared pairs of densely charged ions induce intense but short-range supra-additive slowdown of water rotation. *Phys. Chem. Chem. Phys.* **2016**, *18*, 1918–1930.

(54) Ropp, J.; Lawrence, C.; Farrar, T. C.; Skinner, J. L. Rotational motion in liquid water is anisotropic: a nuclear magnetic resonance and molecular dynamics simulation study. *J. Am. Chem. Soc.* **2001**, *123*, 8047–8052.

(55) Laage, D.; T, H. J. On the residence time for water in a solute hydration shell: application to aqueous halide solutions. *J. Phys. Chem. B* **2008**, *112*, 7697–7701.

(56) Laage, D.; Stirnemann, G.; Hynes, J. T. Why water reorientation slows without iceberg formation around hydrophobic solutes. *J. Phys. Chem. B* **2009**, *113*, 2428–2435.

(57) Stirnemann, G.; Hynes, J. T.; Laage, D. Water hydrogen bond dynamics in aqueous solutions of amphiphiles. *J. Phys. Chem. B* **2010**, *114*, 3052–3059.

(58) Stirnemann, G.; Rossky, P. J.; Hynes, J. T.; Laage, D. Water reorientation, hydrogen-bond dynamics and 2d-ir spectroscopy next to an extended hydrophobic surface. *Faraday Discuss.* **2010**, *146*, 263–281.

(59) Stirnemann, G.; Sterpone, F.; Laage, D. Dynamics of water in concentrated solutions of amphiphiles: key roles of local structure and aggregation. *J. Phys. Chem. B* **2011**, *115*, 3254–3262.

(60) Stirnemann, G.; Castrillón, S. R. V.; Hynes, J. T.; Rossky, P. J.; Debenedetti, P. G.; Laage, D. Non-monotonic dependence of water reorientation dynamics on surface hydrophilicity: competing effects of the hydration structure and hydrogen-bond strength. *Phys. Chem. Chem. Phys.* **2011**, *13*, 19911–19917.

(61) Stirnemann, G.; Laage, D. Communication: on the origin of the non-Arrhenius behavior in water reorientation dynamics. *J. Chem. Phys.* **2012**, *137*, 031101.

(62) Sterpone, F.; Stirnemann, G.; Laage, D. Magnitude and molecular origin of water slowdown next to a protein. *J. Am. Chem. Soc.* **2012**, *134*, 4116–4119.

(63) Xiao, S.; Figge, F.; Stirnemann, G.; Laage, D.; McGuire, J. A. Orientational dynamics of water at an extended hydrophobic interface. *J. Am. Chem. Soc.* **2016**, *138*, 5551–5560.

(64) Laage, D.; Hynes, J. T. Reorientional dynamics of water molecules in anionic hydration shells. *Proc. Natl. Acad. Sci. U.S.A.* **2007**, *104*, 11167–11172.

(65) Moilanen, D. E.; Wong, D.; Rosenfeld, D. E.; Fenn, E. E.; Fayer, M. D. Ion-water hydrogen-bond switching observed with 2D-IR vibrational echo chemical exchange spectroscopy. *Proc. Natl. Acad. Sci. U.S.A.* **2009**, *106*, 375–380.

(66) Ji, M.; Odelius, M.; Gaffney, K. J. Large angular jump mechanism observed for hydrogen bond exchange in aqueous perchlorate solution. *Science* **2010**, *328*, 1003–1005.

(67) Wilkins, D. M.; Manolopoulos, D. E.; Pipolo, S.; Laage, D.; Hynes, J. T. Nuclear quantum effects in water reorientation and hydrogen-bond dynamics. *J. Phys. Chem. Lett.* **2017**, *8*, 2602–2607.

(68) Qvist, J.; Halle, B. Thermal signature of hydrophobic hydration dynamics. *J. Am. Chem. Soc.* **2008**, *130*, 10345–10353.

(69) Rezus, Y. L.; Bakker, H. J. Observation of immobilized water molecules around hydrophobic groups. *Phys. Rev. Lett.* **2007**, *99*, 148301.